75th International Astronautical Congress (IAC), Milan, Italy, 14-18 October 2024.

IAC-24,A6,IP,19,x88756

Targets sequence optimisation for low-thrust multiple active debris removal missions with dynamic programming

Michael Lucchi [a], Giacomo Borelli [a], Camilla Colombo [a]

[a] *Department of Aerospace Engineering, Politecnico di Milano, Via La Masa, 34, Milano, Italy 20156*

Abstract

Over the past few decades, there has been a rapid expansion in the space industry and the number of satellites orbiting Earth. However, this growth has brought to light concerns about the need for active space debris mitigation through removal. In this framework, this paper focuses on the preliminary mission analysis for a low thrust multiple active debris removal mission in Low Earth Orbit (LEO). In the multiple Active Debris Removal (ADR) mission design, the core problem lies in the optimal selection of the mission targets. In this work, a multiple ADR planning tool is developed, which exploits low thrust transfers. The mission architecture proposed is based on a servicer spacecraft visiting the debris once at a time. During the approach and proximity operations, this servicer attaches to the targets a removal kit, then transfers to the next target. The removal kit oversees the deorbiting operations.

The low thrust transfers between the targeted debris in LEO are modelled considering the J_2 perturbed dynamics for near circular orbits. The transfer strategy relies on in plane tangential thrust for the semi-major axis change and out of plane thrusting arcs to match the inclination of the target orbit. The use of intermediate auxiliary drift orbits is included for the Right Ascension of the Ascending Node (RAAN) change, to exploit the effect of the Earth's oblateness in the transfer strategy to optimise the cost. To estimate the transfer time and Δv, a set of analytical solutions for the differential variational equations of the orbital elements is retrieved. This novel low thrust model is coupled with the debris sequence optimisation problem. The analytical nature of the low thrust solutions is instrumental to obtain an efficient algorithm. A dynamic programming method is employed to select the optimal sequence of debris among the provided population, based on a bi-objective metric function of Δv and total time of flight. The developed method was applied to specific rocket bodies and payload debris populations in LEO, orbiting at different inclinations, and the optimal sequences are presented.

Keywords: Debris, Active removal, dynamic programming, low thrust

Nomenclature

	Symbol
Semi-major axis	a
Inclination	i
Right Ascension of the ascending node	Ω
Orbit argument of latitude	u
Earth's gravitational parameter	μ
Earth's oblateness parameter	J_2
Earth's equatorial radius	R_E

Acronyms/Abbreviations

Active Debris Removal	ADR
Low Earth Orbit	LEO
Right Ascension of the ascending node	RAAN
Sun-Synchronous Orbit	SSO
Travelling Salesman Problem	TSP

1. Introduction

1.1 Problem statement

In the last years, there has been a rapid expansion of the space industry, which has caused a great increase in the number of satellites orbiting around Earth. As a consequence of this growth, some concerns about space environment sustainability have been brought to light. The situation is becoming critical, not only for the exponential growth of private space industries, which are now developing great constellations, but also because of the presence of rocket bodies and inoperative orbiting payloads. The Earth's orbit is becoming increasingly crowded, increasing the probability of fragmentation events to occur along with their hypothetical severity. In Figure 1 a graph illustrates the evolution of the space debris population over the years.

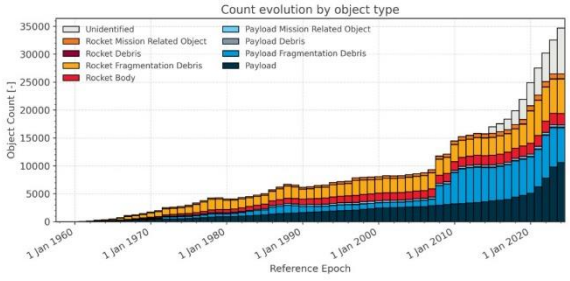

Fig. 1. Space debris objects per type [1]

Recently, ESA has published its "Space Debris Mitigation Requirements" [1], aiming to define the "ESA

Agenda 2025", with the final target of implementing a "Zero Debris" policy by 2030. In the disposal section of the document, not only it is outlined how a non-working satellite should safely re-enter the Earth's atmosphere, but also the requirements and rationale for an Active Debris Removal mission are detailed. In particular, while designing a satellite, it is recommended to implement the required guidelines for its safe removal by an authorised servicer. The formulation of these new policies and requirements clearly demonstrates how the development and implementation of ADR missions are crucial for the future sustainable exploitation of the near-Earth space. Specifically, it will provide an active remediation to the increase of collision risk due to current presence of uncontrolled objects, which will endanger the future in-space operations. As a consequence, it is possible to predict that in the coming years several ADR missions will take place. These missions efficiency is a key to their success, to decrease their cost and have the desired effect on the space industry sustainability. In particular, the number and type of debris to remove need to be defined, the mission architecture, technologies and removal method accordingly, while also considering the trajectory optimisation. Finding the perfect balance of the many possible different combinations of all these aspects is what makes this a great and challenging research branch, which aims at helping the process to make these missions sustainable and worthwhile both environmentally and economically for the space industry.

In this framework, this paper focuses on the preliminary mission analysis for a low thrust multiple Active Debris Removal mission in Low Earth Orbit.

1.2 State of the art

The mission architecture of a multiple ADR mission heavily relies on the satellite platform, removal method, and on the concept of operations. Different possible architectures have been proposed for this kind of mission. The chaser concept is based on a servicer spacecraft which visits all the debris to be removed and performs the removal tasks before visiting the next one. This method has different variants, depending on the removal strategy applied. For example, in Masserini's work [2], it is called "mothership and kits", as the chaser spacecraft was thought as a mothership for the allocation of the removal kits. These are attached to all targets during the proximity operations and then, through different possible techniques, they de-orbit the target. A similar concept has also been analysed by Medioni et al. [3]. This method allows to visit a greater number of debris, but at system engineering level, because of the complexity required to design a spacecraft allocating multiple kits, could be challenging to be developed. In the same work, another chaser concept is studied, for which the removal is performed by the chaser itself. The latter, in fact, after docking to the target debris, performs the de-orbiting and leaves the target on a lower altitude orbit, before going to the next target. In this case, the target de-orbits in time, with a gradual re-entry in Earth's atmosphere. In the "shepherd" concept instead, presented by Wijayatunga et al. [4], the action of two spacecrafts is exploited. When the chaser docked with the space debris reaches a low-altitude orbit, a shepherd spacecraft is launched to de-orbit the debris, while the chaser departs to the next selected target. This concept separates the tasks of rendezvous and docking and the ones for the removal. Clearly, it requires more time to remove the same amount of debris of the chaser and kits concept.

One of the main challenges involved in multiple ADR mission design is represented by the selection of the target debris and by the modelling of the orbital transfers required. This represents an optimisation problem which has two different layers. The first layer involves the trajectory optimisation between couples of debris. The second one, instead, performs the selection of the debris to remove and defines the order in which they have to be visited. The combination of these two topics creates a very challenging framework, as both problems are computationally expensive.

Usually, the transfer layer is formulated through approximate methods that can simplify the transfer design while retaining some level of optimality. The trajectory optimization framework depends mainly on the engine technology used for the transfer. If a high thrust engine is available, an impulsive transfer approximation can be exploited, while if low thrust propulsion is employed, performing an optimization requires the solution of a continuous control problem. In both cases, the trajectory design method must consider the perturbed dynamics of the near Earth environment. Particularly, the most relevant effects is represented by the Earth's oblateness perturbation which causes a continuous drift of the Right Ascension of the Ascending node (RAAN). This aspect in particular makes the optimisation of multiple ADR missions even more challenging, as all the targets are affected by this RAAN drift phenomenon which makes this problem highly time-dependent. On the other side, it can also be exploited strategically to perform some of the required manoeuvres. The most expensive manoeuvres, in fact, are the plane changing ones, specifically those in which the thrust actions are exploited to change the orbit RAAN and inclination. As typically the population of debris to remove is selected conveniently at a similar orbit inclination, to enhance mission efficiency, the RAAN changing manoeuvres remain as the most challenging ones. These usually are performed through auxiliary drift orbits. As the RAAN drift caused by Earth's oblateness is different at different orbit altitudes, an efficient technique consists in changing the orbit semi-major axis, waiting for the differential change of RAAN between the chaser and target, and then

performing a final semi-major axis change to encounter the target. In this way, the orbit plane is changed through in-plane control actions, which are less demanding. The saved cost of the manoeuvres in terms of the required Δv impulse results in an increase of the manoeuvre duration, because of the waiting time spent on the drift orbit.

Once the method for the trajectory optimization is selected, the problem becomes a matter of selecting the optimal path for the servicer. This is defined in many papers as a travelling salesman problem (TSP), which, in this case, due to the effect of Earth's oblateness, usually becomes a time dependent travelling salesman problem (TDTSP). The objective is to find the most efficient path to visit all the targets of the mission. The approaches to solve this problem can be subdivided into deterministic and heuristic methods. Deterministic methods are computationally heavy, as they explore the totality or the majority of the possible available solutions, but they guarantee the optimality of the solution obtained. Heuristic methods instead are employed for bigger problems, as they have an evolutionary-based logic to find the solution to the problem. Despite the advantages, while they may be faster than deterministic algorithms, they do not guarantee the optimality of the solutions, and they can converge to different solutions at each iteration. Selecting among deterministic methods, the algorithms which can be used to solve the TDTSP are the brute force, the branch and bound and the dynamic programming. The brute force algorithm is the simplest and heaviest of the three algorithms. It considers all the possible path combinations, selecting the best one in the end. The branch and bound algorithm works similarly, but while developing the tree of possible solutions, a bound function evaluation excludes the branches which are not promising, reducing the total computational cost. Dynamic programming instead reduces the computational cost solving locally the decision problem at each step of the path, and finding the optimal solution exploring the less possible solution branches. This approach has been used by Campiti [5] for the optimisation of resonant flybys, where the decision-making problem was to select the semi-major axis of the subsequent flyby orbits.

Heuristic methods instead can present different versions, based on evolutionary theories of natural phenomena. The genetic algorithm is the most explored heuristic method and has a great variety of possible applications. When applied on path selection problems, this algorithm is based on creating an initial population of possible solutions, then through crossing over and mutation functions, this population evolves through generations searching for the most efficient solution. Exploring past works about multiple ADR, there have been several different approaches, which mainly differ for mission architecture and targets, trajectory optimization strategy and algorithm for the path selection. Cerf [6], for example, has considered a specific set of four impulsive manoeuvres consisting of 2 Hohmann transfers, with an additional waiting time on the intermediate drift orbit. Then, the debris sequence is optimized through a branch and bound algorithm, with the objective of minimizing the total Δv, starting from a good initial guess and reaching stable feasible solutions in few iterations. Although, as reported in the work conclusions, the method suits perfectly for small or medium debris populations size, while it is difficult and costly to be applied for larger size problems. His work can be considered an evolution of the one from Madakat et al. [7], which used the same combinatorial path algorithm and a Lambert based transfer strategy. The two works differ as in the latter the perturbations caused by Earth's oblateness during the transfers were neglected. Moreover a bi objective optimisation based on the total Δv and the transfer time was considered. Al Naber, in his work [8], similarly performs the debris sequence optimisation through the exploitation of high thrust impulsive manoeuvre and a branch and bound algorithm. Interestingly, he uses a particular method to select and optimise the sequence of debris. In fact, the index of merit for the selection not only accounts for the mission cost in terms of Δv, but also evaluates the environmental and operability indexes for the target debris. Masserini instead applies a similar strategy to a different population. In his work [2] he exploited a branch and bound algorithm to evaluate different mission architectures feasibility for failed constellation satellites removal. Another work based on the branch and bound algorithm has been carried out by Barea et al. [9], who developed a two-level algorithm. In the upper level, a subset of a large pool of candidate is identified, while in the lower level the trajectory path and order in which they have to be visited is finally defined. Barea et al. [10] also produced a work on ADR constellations. In this work constraint programming, an classical and flexible artificial intelligence paradigm, is employed for the multiple ADR sequence optimisation of failed constellation satellites. As done by the majority of the aforementioned works, a chaser and kits architecture is considered. In the field of low thrust trajectory optimisation strategies instead, an interesting work has been produced by Di Carlo et al. [11]. In the paper, the objective is to define the most efficient ADR strategy. Two different concept are analysed. The first concept is the chaser and kits concept, while in the second concept the chaser docks with the targets and then performs itself the de-orbiting operations. Di Carlo et al. use a simple but powerful heuristic algorithm that can solve complex discrete decision-making problem, based on the Physarum Polycephalum organism. For the low thrust optimisation instead, Di Carlo applied the theoretical model developed by Zuiani and Vasile [12], who obtained an average analytical formulation for the

perturbing accelerations acting on the spacecraft during multiple revolutions low thrust spirals. The strategy for the transfer exploits a drift orbit for the RAAN change to match the target RAAN, on which the spacecraft positions after matching the other orbital elements of the target. In the end, the de-orbiting kit attachment concept is proven to be the most efficient. Hon and Emami [13] interestingly apply a different method to the same debris population used by the aforementioned Di Carlo's paper. This method applies a combination of an analytical estimation method with a Q-Law inspired guidance scheme. Then, it searches for the path solution through a genetic algorithm and finally refines the solution through a gradient-based method to tune the gains in the Lyapunov function used by the Q-Law method, finding very promising solutions. An important contribution about low thrust optimisation can be found in Huang's work [14] about the mission analysis of low thrust satellite constellations. In this work, the variational equations of the orbital elements for near circular orbits are solved analytically. This offers a particularly interesting framework if applied in to the multiple ADR mission design, as having analytical solutions for the optimisation of every transfer could speed up the successive path selection algorithm. Braun et al. [15] finally offer an interesting comparison between chemical and electric propulsion, applying them to the accomplishment of the same mission. As a result, chemical propulsion appears clearly faster in performing the same tasks, while electric propulsion allows for a reduced propellant mass, resulting in an higher efficiency.

1.3 Paper scope

In this work a low thrust propulsion technology is selected for the multiple ADR mission. The objective of this work is to develop a low thrust trajectory optimisation method with a low computational load, to be included in a dynamic programming scheme to select the ADR targets to be removed among a greater population, estimating the mission cost. The low thrust trajectory optimisation model is inspired by Huang's work [14]. A dynamic programming algorithm is then developed to solve the path selection and optimisation problem. The transfers are optimised by means of a cost function featuring a combination of the Δv and time of flight. Then, a preliminary mission analysis for the trajectory optimisation of a generic multiple active debris removal mission in LEO will be performed. The debris population, in particular, will include debris with similar characteristics between them and with a certain relevance for the space debris problem. This research aims at developing an efficient mission planning tool which exploits analytical methods for low thrust transfers and dynamic programming for the sequence selection.

The novelty of this work with respect to the mentioned past works is the combination of these two computationally efficient frameworks. The mission architecture is carefully planned and modelled to exploit the RAAN drift caused by the J_2 perturbation on the LEO orbital dynamics. The dynamic programming algorithm is expected to select the optimal debris combination to strategically take advantage of the mission transfers model.

2. Space Debris population in LEO

The open-source data from ESA DISCOSweb [16] are used to analyse the current debris population. This data were taken on December 1st 2023. In order to select a valuable population for the study, it is decided to analyse a group of debris orbiting at an altitude between 500 km and 2000 km, and with a low level of eccentricity ($e < 0.1$). The lower limit is selected to exclude debris which are predicted to re-enter the atmosphere passively in a short period of time, while the upper one is the limit of LEO. The selected population is divided into two main categories, as reported in Table 1. These are rocket bodies and payloads. Rocket bodies are the launchers upper stages remained in orbit, while payloads are satellites which performs measurements in space through specific instruments and constellation satellites.

Table 1. Space Debris Population types: 01-12-2023.

	Number
Rocket Bodies	791
Payloads	823
TOTAL	1614

The distribution of payloads and rocket bodies in LEO is displayed in Figures 2 and 3. Starting from the semi-major axis distribution, which is taken as the x-axis for all the figures, it is clear that both rocket bodies and payloads mainly concentrate in the area below 7500 km. Analysing the orbit inclination, it is possible to see clusters of rocket bodies and Sun Synchronous Orbit (SSO) payloads concentrating around 100◦, at low altitudes. For the payloads, the Globalstar constellation cluster can be identified around an inclination of 50◦. This is confirmed also by the mass distribution, showing equal mass satellites in the same region. The vast majority of rocket bodies and payloads mass stays below 2000 kg, even if some rocket bodies, which are the Russian Zenit launcher second stages, have masses up to 9000 kg.

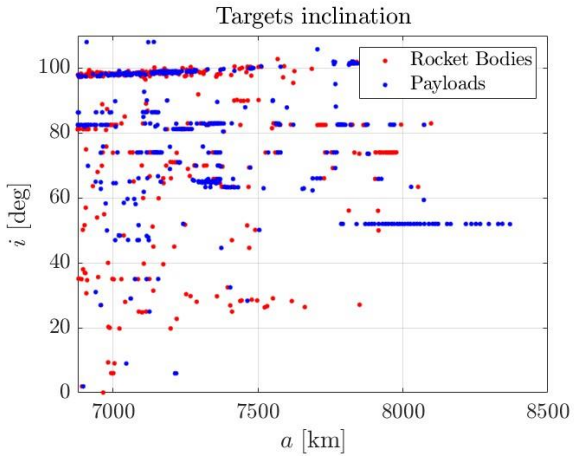

Fig. 2. Debris population inclination vs semi major axis.

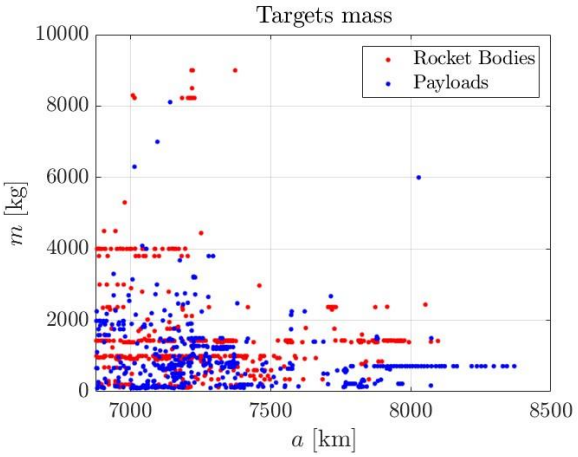

Fig. 3. Debris population mass vs semi-major axis.

3. Mission architecture

3.1 Mission concept of operations

The mission architecture used for this research is based on the chaser and kits concept. The chaser is a servicer spacecraft which performs all the transfers from one debris to the other, while the removal kits are attached to the targets during the target approach. The propulsion technology selected for the servicer is electric propulsion, which results in a low-thrust level available for the transfers. The chaser is assumed to be released in proximity of the first selected target, in order to perform the first removal. Then, it performs every transfer sequentially. The de orbiting kits are considered to have all equal mass. This work does not concentrate on the proximity operations phase or on the technique used for the removal and the sizing of these kits.

3.2 Low thrust analytical model

The strategy employed to design the low-thrust transfer is based on previous works by Huang [14]. The orbital dynamics considered is formulated with the Gauss variational equations including the J_2 perturbation due to the Earth's oblateness. Accordingly, the Keplerian elements rates can be written as follows:

$$\dot{a} = \frac{2f_t}{n} \quad (1)$$

$$i = \frac{f_h}{na}\cos u \quad (2)$$

$$\dot{\Omega} = \frac{f_h}{na}\frac{\sin u}{\sin i} - \frac{3nJ_2{R_E}^2}{2a^2}\cos i \quad (3)$$

where f_t and f_h are respectively the in-plane tangential and out-of-plane accelerations, n is the orbit mean anomaly, a is the orbit semi major axis, i is the orbit inclination, u is the argument of latitude. J_2 is the Earth's oblateness parameter and R_E represents the Earth's equatorial radius. The equations are not reported for the eccentricity and argument of latitude as the satellites orbits are considered to be near-circular and the phasing operations are neglected. Having to model the transfer between two generic satellites, a suitable transfer model is built to exploit the aforementioned equations.

A strategy aiming at matching the three orbital elements appearing in the above equations is developed. In particular, the following mission phases, which are performed sequentially, can be identified:

1. In-plane thrust transfer to a drift orbit: the services selects an optimal drift orbit semi major axis;
2. Out-of-plane thrust orbit inclination change: the target orbit inclination is matched;
3. RAAN matching drift orbit waiting: the services waits on the drift orbit to exploit the differential RAAN drift with the target;
4. In-plane thrust final orbit matching: the target orbit is matched completely.

These phases physical modelling is presented in the following sections

3.3 In-plane thrust transfer to a drift orbit

During this first phase, the in-plane thrust is applied only tangentially with respect to the spacecraft velocity, obtaining a change in the orbit semi-major axis. This aims at reaching the drift orbit RAAN change rate caused by the J_2 perturbation. Fixing the objective Δa as:

$$\Delta a = a_d - a_0 \quad (4)$$

where a_0 and a_0 are the drift orbit and initial orbit semi-major axis, the Equation 3.2 can be integrated to obtain the time of flight needed to perform this transfer phase, as taken by Huang's work [14] :

$$\Delta t_1 = \frac{m_0}{\dot{m}}\left\{exp\left[\frac{\dot{m}}{F\ sgn(\Delta a)}\left(\sqrt{\frac{\mu}{a_0}} - \sqrt{\frac{\mu}{a_d}}\right)\right] - 1\right\} \quad (5)$$

where m_0 is the spacecraft mass at the beginning of the transfer, $\dot{m}$ is the engine exiting mass flow rate, F is the engine thrust and μ is the Earth's gravitational constant. The effect of this transfer manoeuvre reflects also on the RAAN drift, as the J_2 effect has to be integrated along the trajectory. In fact, as the semi-major axis constantly changes, the perturbation is not constant during the transfer. Accounting for this effect and knowing the final spacecraft mass m_1, integrating the equations along the trajectory, it is possible to track the RAAN change for the chaser during the manoeuvre.
Finally, it is also possible to compute the required impulse, in terms of Δv, through the following.

$$\Delta v_1 = \frac{F}{\dot{m}} \ln\left(\frac{m_1}{m_0}\right) \quad (6)$$

3.4 Out-of-plane orbit inclination change
After the transfer to the drift orbit, the inclination change manoeuvre is performed to match the target one. In order to model this manoeuvre, the approach followed by Huang [14] is taken as an inspiration. In particular, the out-of-plane thrust is applied during the passages at the orbit nodes, following this logic:

$$f_h = \begin{cases} +sgn(\Delta i)(F/m), & -\eta < u < \eta \\ +sgn(\Delta i)(F/m), & \pi - \eta < u < \pi + \eta \\ 0, & otherwise \end{cases} \quad (7)$$

where $sgn(\Delta i)$ represents the sign of $\Delta i = i_T - i_C$, with i_T and i_C being the target and chaser orbit inclinations. η is instead the transfer arcs amplitude. For this work, a value of η = 25° is selected. Integrating the equations, it is possible to retrieve the time of flight for this second phase:

$$\Delta t_2 = \frac{\pi m_1}{2\dot{m}\eta} \left\{ exp\left[\Delta i \frac{\eta}{\sin\eta} \frac{n_d a_d \dot{m}}{sgn(\Delta i) F} \right] - 1 \right\} \quad (8)$$

As before, the impulse Δv_2 is retrieved through the computation of the used propellant mass, accounting for the fact that intermittent out of plane thrusting arcs are applied

$$\Delta v_2 = \frac{F}{\dot{m}} \ln\left(\frac{m_2}{m_1}\right) \quad (9)$$

3.5 RAAN matching waiting
The third phase is a waiting phase on the drift orbit, which semi-major axis is the target of the first in-plane manoeuvre. This auxiliary orbit is the principal feature of this transfer optimisation, as it will be explained in section 3.7. As it can be deduced by Equation 3, the J_2 perturbation effect depends on the orbit semi-major axis. Exploiting the difference between the drift and target orbit semi-major axes, the waiting time on the drift orbit can serve as a free RAAN matching manoeuvre. In order to compute this waiting time, it is important to define the RAAN difference $\Delta\Omega$ and the RAAN rate difference $\Delta\dot{\Omega}$ between the target and the chaser.
Starting from $\Delta\dot{\Omega}$, it is easily determined as:

$$\Delta\dot{\Omega} = \dot{\Omega}_T - \dot{\Omega}_C \quad (10)$$

where $\dot{\Omega}_T$ and $\dot{\Omega}_C$ are determined through Equation 3, clearly considering only the natural drift contribution, as during this phase thrust is not applied. Regarding $\Delta\Omega$, it is important to remember the objective of this phase.
In particular, the overall objective of this manoeuvre is not to equal the chaser and target RAAN at the end of the waiting time, but at the end of the transfer phases. This translates into considering the different RAAN drifting contributions that they will experience during phase 4.
In fact, the target RAAN continues changing constantly during phase 4 due to the J_2 perturbation effect, according to its semi-major axis. For the chaser instead, the effect of the manoeuvre yet to be performed, namely the one to change its semi-major axis to finally match the target orbit one, has to be taken into account. Moreover, also the different RAAN change contributions developed during phase 2 have to be taken into considerations. In fact, after the semi-major axis change, the differential RAAN variation between the chaser and target begins. It is worth remarking that the inclination in Equation 3 is considered constant during the averaging procedure. In particular, the value taken is the average along the manoeuvre duration. The $\Delta\Omega$ between chaser and target to obtain results as:

$$\Delta\Omega = \Omega_{T4} - \Omega_{C4} \quad (11)$$

where Ω_{T4} and Ω_{C4} are the target and chaser RAAN computed considering as starting point the end of phase 2 and the different RAAN drifting contributions that they will experience during phase 4. In this way, the $\Delta\Omega$ to be accomplished during phase 3 is computed.
An additional complexity in the design of this manouvre lies in the signs of $\Delta\Omega$ and $\Delta\dot{\Omega}$, computed confronting the drift and target orbits. In fact, selecting the drift orbit semi-major axis implies the selection of a sign for the $\Delta\dot{\Omega}$, which has to be the right one for the two orbits $\Delta\Omega$. Depending on the orbit inclination, which determines the westward or eastward direction of the RAAN drift, and the sign of $\Delta\Omega$, the following different cases can be identified.
Starting from the prograde orbits cases, for which the RAAN drifts westward, decreasing its value, the cases reported in Figures 4 and can verify. In particular, the

four cases include all the possible combination for the $\Delta\Omega$ and $\Delta\dot{\Omega}$ signs.

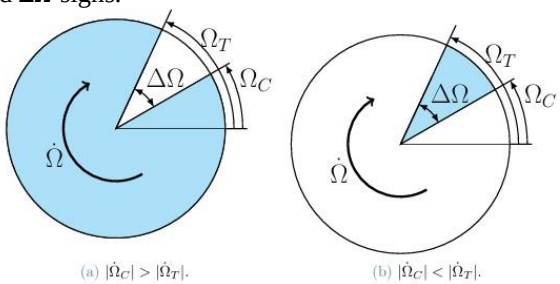

Fig. 4. Prograde orbits: $\Delta\Omega > 0$.

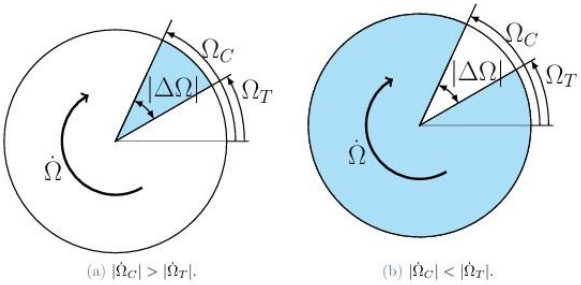

Fig. 5. Prograde orbits: $\Delta\Omega < 0$.

In Figure 4, a positive $\Delta\Omega$ is considered. In this case, depending on the relation between the drift and final orbit semi-major axis, the waiting time on the drift orbit can be computed as:

$$\Delta t_3 = \begin{cases} \frac{2\pi - \Delta\Omega}{|\Delta\dot{\Omega}|}, & |\Delta\dot{\Omega}_C| > |\Delta\dot{\Omega}_T| \\ \frac{\Delta\Omega}{|\Delta\dot{\Omega}|}, & |\Delta\dot{\Omega}_C| < |\Delta\dot{\Omega}_T| \end{cases} \tag{12}$$

In Figure 5 instead, a negative $\Delta\Omega$ is considered. In this case, the waiting time on the drift orbit results as:

$$\Delta t_3 = \begin{cases} \frac{|\Delta\Omega|}{|\Delta\dot{\Omega}|}, & |\Delta\dot{\Omega}_C| > |\Delta\dot{\Omega}_T| \\ \frac{2\pi - |\Delta\Omega|}{|\Delta\dot{\Omega}|}, & |\Delta\dot{\Omega}_C| < |\Delta\dot{\Omega}_T| \end{cases} \tag{13}$$

Considering retrograde orbits cases, for which the RAAN drifts eastward, increasing its value, the cases reported in Figures 6 and 7 are identified.

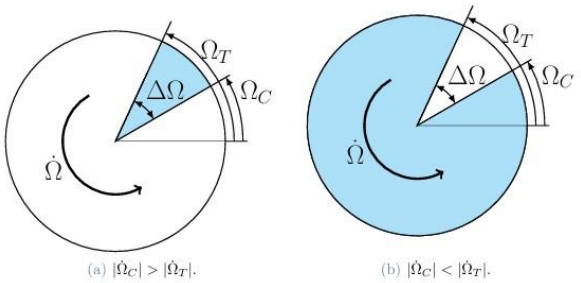

Fig. 6. Retrograde orbits: $\Delta\Omega > 0$.

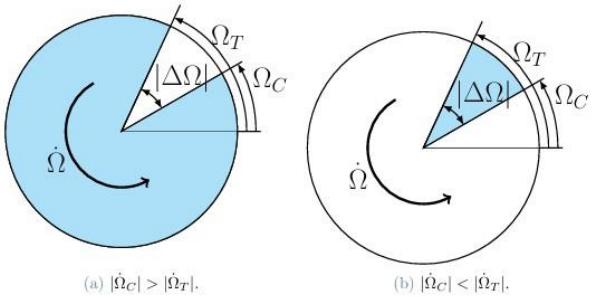

Fig. 7. Retrograde orbits: $\Delta\Omega < 0$.

In Figure 6, a positive $\Delta\Omega$ is considered. The waiting time on the drift orbit can be computed as:

$$\Delta t_3 = \begin{cases} \frac{|\Delta\Omega|}{|\Delta\dot{\Omega}|}, & |\Delta\dot{\Omega}_C| > |\Delta\dot{\Omega}_T| \\ \frac{2\pi - \Delta\Omega}{|\Delta\dot{\Omega}|}, & |\Delta\dot{\Omega}_C| < |\Delta\dot{\Omega}_T| \end{cases} \tag{14}$$

In Figure 7 instead, a negative $\Delta\Omega$ is considered. In this case, the waiting time on the drift orbit results as:

$$\Delta t_3 = \begin{cases} \frac{2\pi - |\Delta\Omega|}{|\Delta\dot{\Omega}|}, & |\Delta\dot{\Omega}_C| > |\Delta\dot{\Omega}_T| \\ \frac{|\Delta\Omega|}{|\Delta\dot{\Omega}|}, & |\Delta\dot{\Omega}_C| < |\Delta\dot{\Omega}_T| \end{cases} \tag{15}$$

3.6 In-plane thrust orbit matching

The final manoeuvre to occur is the same in-plane tangential thrusting manoeuvre performed at the beginning. It is exploited to change the semi-major axis from the drift orbit value to the target value. Following the same procedure explained in Section 3.3, starting from the computation of Δa:

$$\Delta a = a_f - a_d \tag{16}$$

The time of flight is computed as:

$$\Delta t_4 = \frac{m_3}{\dot{m}} \left\{ exp\left[\frac{\dot{m}}{F\ sgn(\Delta a)} \left(\sqrt{\frac{\mu}{a_d}} - \sqrt{\frac{\mu}{a_f}} \right) \right] - 1 \right\} \quad (17)$$

where m_3 is the spacecraft mass at the beginning of the transfer. The effect of this transfer manoeuvre, as anticipated in section 3.3, reflects also on the RAAN drift. This effect is computed and taken into account for the procedure explained in Section 3.5.
As previously done, the required impulse can be retrieved, in terms of Δv, through the following.

$$\Delta v_4 = \frac{F}{\dot{m}} \ln\left(\frac{m_4}{m_3}\right) \quad (18)$$

3.7 Cost Function and Optimisation parameter

The transfer strategy previously described is fully defined upon selecting one key variable: the drift orbit semi-major axis. In particular, a weighted parameter x representing the semi major axis difference between the drift orbit and target orbit semi-major axis, divided by the latter, is selected.

$$x = \frac{\Delta a}{a_f} = \frac{a_0 - a_f}{a_f} \quad (19)$$

Once the parameter to be defined is selected, the rationale behind its selection and optimisation is defined. In particular, considering the mission cost, it is decided to take into consideration the time of flight and the impulse Δv. The cost function is defined as follows:

$$J(x) = \beta \frac{\Delta v_i(x)}{\Delta v_{TOT}} + (1-\beta) \frac{\Delta TOF_i(x)}{\Delta vTOF_{TOT}} \quad (20)$$

where β represents a weighting parameter defined to prioritise differently the contributions to the cost function.

3.8 Sensitive study: initial guess refinement

The implementation of the trajectory optimisation procedure is carried out through the MATLAB *fmincon.m* function and using its sequential quadratic programming algorithm. It is observed that the definition of the parameter x can cause the transfer to fall into the different scenarios for the drift orbit optimisation, regarding the signs of $\Delta\Omega$ and $\Delta\dot{\Omega}$. It can be pointed out that the simultaneous presence of more than one scenario in some areas where the optimisation is performed results in the MATLAB function not to converge to the real optimal solution. In Figure 3 an example of this phenomenon is represented.

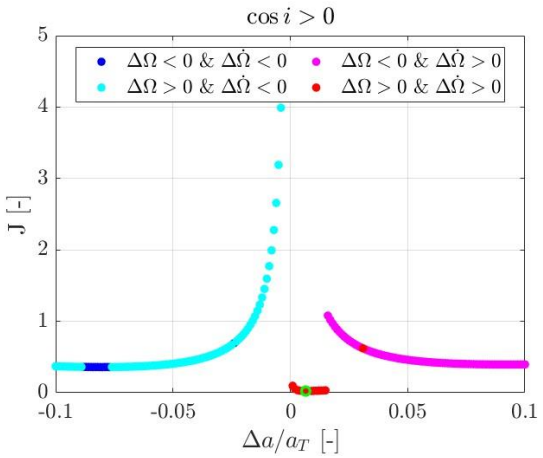

Fig. 8. Mission cost J varying x: prograde orbit.

In order to solve this problem and refine the model, two features are added to the optimisation process. Firstly, an initial screening on x is performed, to identify a generic minimum and its relative scenario. Then, the optimiser is launched using as initial guess the found minimum, and bounded around its value. Moreover, a constraint function is designed to force the optimisation function to find the optimisation solution in the same scenario identified for the minimum. The results of this process can also be seen in Figure 8, where the optimal solution found by the solver is indicated by the green circle.
A sensitive study of the optimisation problem behaviour is performed, selecting an initial LEO orbit and solving the optimisation for transfers to neighbouring orbits.
In particular, as initial condition a = 7800 km, i = 63◦ and Ω = 180◦ are taken. Then, a grid of initial targets Δa and $\Delta\Omega$ ranging between −500 km and +500 km and between −60° and 60° is created, assuming the chaser and target orbit inclination as equal. The optimisation procedure explained in this section is applied for each possible transfer destination and the results for the mission cost are reported in Figure 9. Two main features are observed. Firstly, it is clear that the plane changing manoeuvres are more impacting on the mission cost with respect to the in-plane manoeuvres. In fact the cost function has a more steep increase on the $\Delta\Omega$ axis. The second feature which can be observed is that there is a minimum region spanning from the positive $\Delta\Omega$ and negative Δa region to the negative $\Delta\Omega$ and positive Δa region. This suggests that the combination of the $\Delta\Omega$ and Δa in the mentioned region is particularly advantageous, as the RAAN drift caused by the Δa initial condition helps cover the required $\Delta\Omega$ to be performed.

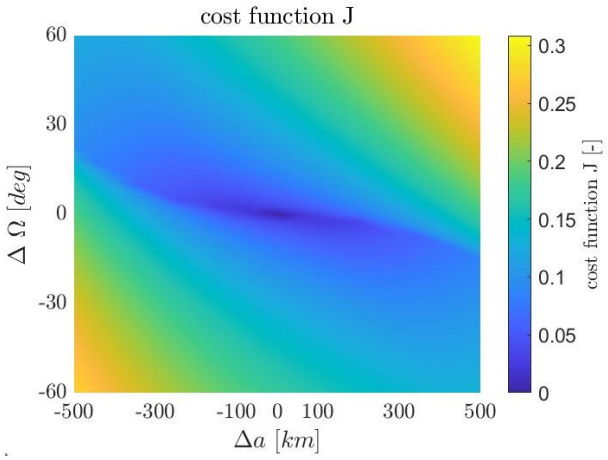

Fig. 9. Mission cost J varying x: prograde orbit.

4. Dynamic programming

Dynamic programming is a decision making algorithm for multi-stage problems, where each decision to be made influences the outcome of the next steps. In fact, typically, to configure a dynamic programming application, it is important to define stages and states and a decision to be made at each stage. For multiple ADR trajectory design, the stages of the problem are identified as the transfers to be performed between the debris. The states to select are instead the target debris orbits in which the servicer could lie at the end of each transfer. The decision to be made at each stage is the selection of the debris to visit next. Making these decisions, following the trajectory optimisation procedure, consists in minimising the defined cost function for each transfer.

4.1 Assumptions

The algorithm has the objective to select and order a sequence of space debris to be removed during the mission, taken from a greater population of debris. Dynamic programming allows to compute the optimal sequence, as the transfer optimisation is performed at each step. The assumptions are:

• The transfers are performed following the strategy proposed in Section 3;
• The engine operational qualities are considered constant throughout the whole mission;
• The de-orbiting kit and the propellant mass used for each transfer is subtracted by the spacecraft mass after each removal is per formed;
• The number of debris to be removed N is fixed a priori.

4.2 Dynamic programming algorithm

Here below the steps taken by the algorithm are explained. For every possible choice of the first debris, the optimisation starts after its removal, following the same steps:

1. Starting from the selection of the second debris, the trajectory optimisation procedure explained in Section 3 is applied for each possible target remained. A local problem optimisation is solved at each step to find the minimum transfer cost. Only the best local solution is saved and the optimisation continues for each step, starting each time from the last visited debris.

$$J_{i,1}^* = J_{i,1}(s_{i,0}, x_j^*) = \min J_{i,1}(s_{i,0}, x_j) \quad (21)$$

where $s_{i,0}$ is the initial state of the spacecraft, corresponding to the orbit of the first debris selected, referred to as the i-th debris, as the same procedure is repeated for each debris. The state x_j instead represents a generic arrival debris initial state. The state x_j^* is the selected debris for the first transfer, which represents the one minimising the cost function J. The mission cost $J_{i,1}^*$ is the minimised cost function evaluation for the sequence starting at the i-th debris, at the end of the 1st stage.

2. From the second stage to the N-th stage, the RAAN drift of all debris has to be taken into account. This means that the remaining states x_j change at each stage k of the algorithm. In particular, their RAAN drifts according to the natural drift.

$$\Omega(x_j, k) = \Omega(x_j, k-1) - \frac{3nJ_2{R_E}^2}{2a^2}\cos i\, \Delta t_k \quad (22)$$

where a and i are the semi-major axis and inclination of the debris corresponding to the state x_j. The drift time Δt_k is retrieved from the total cumulative time of flight at the corresponding k-th stage, which data is collected and saved for all the optimal paths, as well as the propellant mass used and impulse Δv.
This way, for each stage k:

$$J_{i,k}^* = J_{i,k-1} + J_{i,k}(s_{i,k-1}, x_j^*) \quad (23)$$

with $J_{i,k-1}$ being the optimised mission cost for the sequence starting from the the i-th debris at the k-th stage and:

$$J_{i,k}(s_{i,k-1}, x_j^*) = \min J_{i,k}(s_{i,k-1}, x_j) \quad (24)$$

where $s_{i,k-1}$ is the state before the k-th stage decision and x_j represents one of the possible decisions composing the set S_j, clearly excluding the debris that have already been visited. x_j^* is the optimal decision made at each stage.

3. In the end, once N optimal sequences are defined, the one having the most efficient mission cost is selected.

$$J = \min J_i \quad (25)$$

5. Test cases and results

5.1 Mission Data and Test cases population

The ADR mission data for the servicer employed in the simulations is reported in Table 2. It is decided to run the algorithm for different sub groups of space debris taken by the population analysed in Section 2. The further assumptions made to restrict the debris populations are to select near circular orbits (e < 0.001) and to take debris with a mass between 700 and 2000 kg. This range is selected to make the targets mass compatible with the removal kit mass. Two main clusters are analysed. The first one orbits at the typical inclinations of the SSO, between 90° and 100°, while the second lies in the inclination region around 50°, composed mainly by inactive satellites of the Globalstar constellation. These two clusters, comprehending respectively 34 and 37 debris, are taken as two separate test case populations. It is selected to remove a sequence of N = 5 debris in both cases.

Table 2. Mission parameters and data.

	Symbol	Value
Spacecraft initial mass	m_0	2750 kg
Removal kit mass	m_{kit}	175 kg
Engine thrust	F	100 mN
Engine specific impulse	I_{sp}	2000 s
Mission duration	TOF_{TOT}	3 years
Mission available impulse	Δv_{TOT}	2 km/s
J weighting parameter	β	0.5

5.2 Results

The simulations are run on a computer having as processor an Intel(R) Core(TM) i7-7500U CPU @ 2.70GHz- 2.90 GHz, with an installed RAM of 8 GB. The solutions for both population test cases are reported in Table 3, with the computational time t_c.

Table 3. Population results: test case 1 and 2.

Case	Size	Δv	TOF	t_c
1	34	0.3728 km/s	252.8 d	56.1 s
2	37	0.2262 km/s	194.2 d	123.1 s

5.2.1 Results analysis: test case 1

In Figure 10 a breakdown of the transfers for the solution of the first test case is given, representing the chaser and targets RAAN evolution during the transfers. In particular, the chaser RAAN evolution is represented throughout all the transfers, while the targets RAAN evolution is represented only for the relative transfer arcs in which they are the actual target. Here the RAAN is represented just showing the initial and final values for each transfer. Two main phenomena can be observed. First, it can be seen that the targets are selected in order to have a little initial RAAN value separation with respect to the chaser. In fact, in the figure, the target at chaser RAAN curves can hardly be distinguished. This is caused by the fact that the RAAN matching manoeuvre is the most demanding in terms of mission cost, and the algorithm manages to select the target which helps minimise this cost. Then it can be seen that, as the population of the first test case orbits Earth on retrograde orbit, their RAAN drift is positive during the mission time.

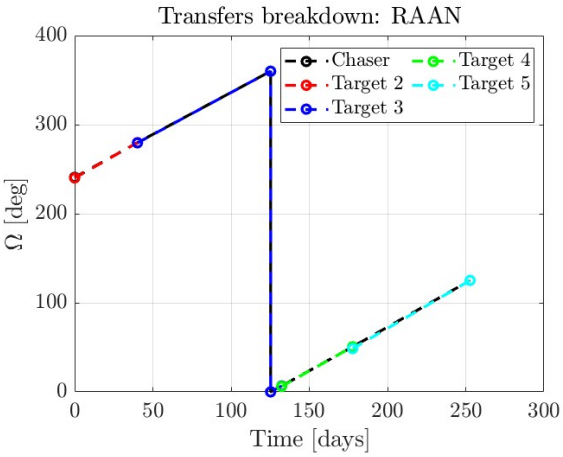

Fig. 10. Transfers RAAN evolution: test case 1.

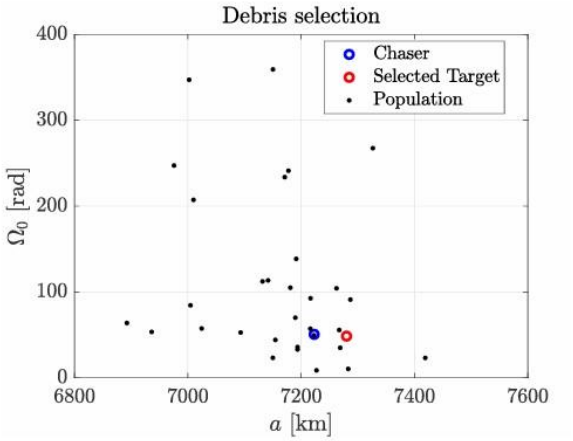

Fig. 11. Final debris selection: test case 1.

In order to get more insight on the single debris-to-debris transfers, in Figure 11, the population debris semi-major axis and RAAN values just before the choice of the final debris are reported. It can be pointed out that, despite the distance in semi-major axis, the selected target is chosen mainly due to the similarity in RAAN with the chaser.

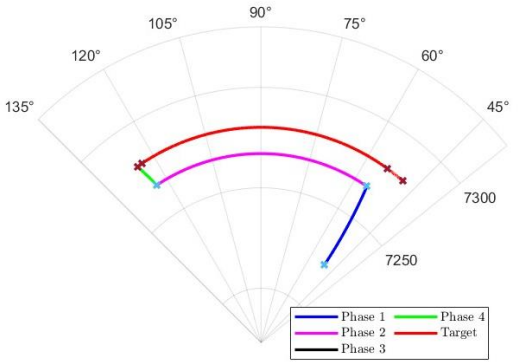

Fig. 12. Fourth transfer phases: RAAN vs a polar plot.

Interestingly, the target has a lower RAAN but an higher semi-major axis and in Figures 11, the reasons of this choice can be retrieved. This polar plot represents the semi-major axis and RAAN evolution through the four different mission phases. Crosses and circles represent the time instant at the beginning and end of each transfer phase. These instants are reported also for the target, to give a comprehensive view of the situation. In this transfer the chaser chooses to increase its semi-major axis to reach the drift orbit. By moving at higher altitudes, the chaser tunes its RAAN drift with respect to the target RAAN drift, to help the RAAN matching at the end of the mission. Another feature can be seen in the figure. The phase 3 of the transfer, which consists of the waiting time on the drift orbit, is almost absent, due to the fact that it is performed during phase 2. The drift orbit semi-major axis is, in fact, reached before phase 2. During the inclination changing phase, as a consequence, the chaser has already the desired differential RAAN change with the target designed for phase 3. As the inclination change is usually the most demanding manoeuvre, the positioning of phase 2 after reaching the drift orbit is strategic for the purpose of optimising the waiting time of phase 3.

5.2.2 Results analysis: test case 2

Analysing the test case 2 results, in Figure 13, two other features of the RAAN drift can be noticed. Firstly, as in this case the population orbits Earth on prograde orbits, it can be seen that the RAAN drift is negative during the mission time. Moreover, it can be noticed that the RAAN drift is faster with respect to what observed for test case 1. This is mainly due to the orbit inclination. In fact, the RAAN drift depends on the cosine of the inclination, which, for the values selected, results much greater for the test case 2 population. As previously done, to analyse better the single debris-to-debris transfers, in Figure 14, the population debris semi-major axis and RAAN values just before the choice of the fourth debris are reported. In this case the selected target results the nearest in the graph, both in terms of RAAN and semi-major axis.

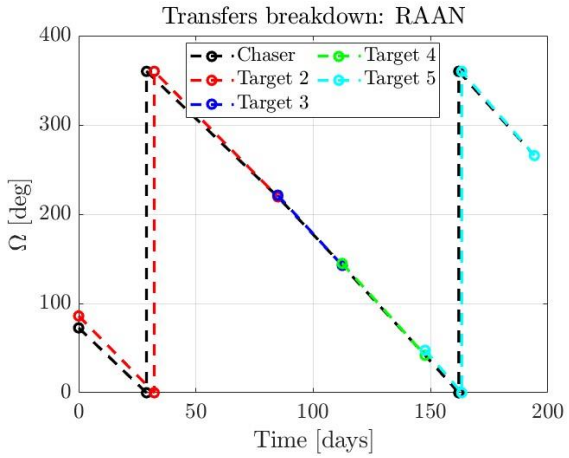

Fig. 13. Transfers RAAN evolution: test case 2.

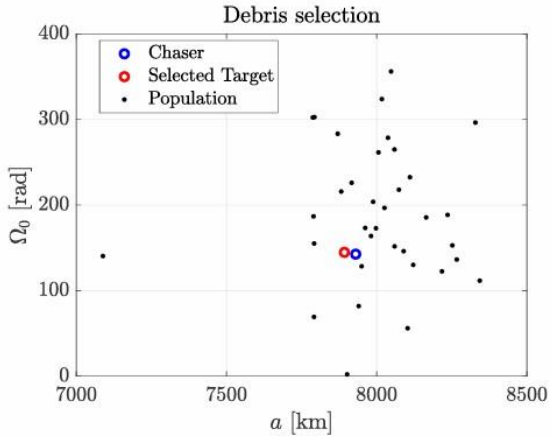

Fig. 14. Fourth debris selection: test case 2.

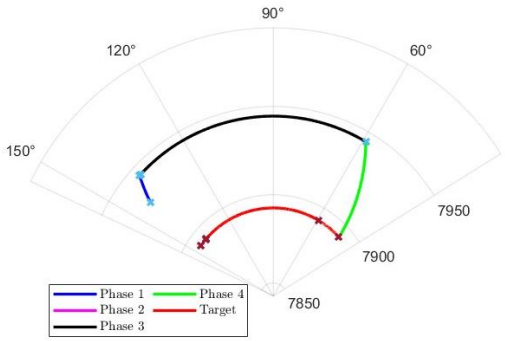

Fig. 15. Third transfer phases: RAAN vs a polar plot.

It can be observed that the target has a lower semi-major axis but higher RAAN and in Figure 15, a more deep view into this choice can be made, reporting the polar plot and RAAN evolution of the transfer, as done in Section 5.2.1. Similarly to what observed before, the chaser chooses to increase its semi-major axis to reach the drift orbit. The difference with the case analysed in test case 1, however, is that, in this case, slowing down its RAAN drift is instrumental to match the target RAAN from a

lower value, while in the previous case this helped matching it from a higher value. This shows again the different behaviours of RAAN drift phenomena for prograde and retrograde orbits. Another difference with the transfer shown in test case 1 is that this time phase 2 is almost absent, due to the fact that the target and chaser inclination are almost equal. This helps appreciate better the effect of the RAAN waiting time of phase 3, as the RAAN evolution can be appreciated in the polar plot of Figure 15.

6. Conclusions

This work presents a fast and computationally efficient method for the trajectory and sequence optimisation of low thrust multiple ADR missions. Starting from the analysis of the current space debris population in LEO, compatible clusters of possible targets for a multiple ADR mission were identified and evaluated. Then, the two main layers regarding the nature of the multiple ADR trajectory and targets optimisation were addressed. Starting from the trajectory optimisation, the mission architecture and assumptions were defined. It was decided to select a low thrust propulsion technology, to increase the mission efficiency, and to explore the possibility of modelling the low thrust transfers in a computationally efficient way for the targets optimisation framework. The transfer strategy was designed for near-circular orbit applications and divided in four main phases, modelled with a J_2 perturbed dynamics. This strategy relies on the exploitation and optimisation of intermediate drift orbits aiming at exploiting the differential RAAN drift caused by Earth's oblateness to perform the RAAN matching manoeuvres of the single debris to debris transfers. The low thrust analytical model, inspired by Huang's work [14], has been discussed and developed, expanding its application to the inclination change manoeuvre. Through analytical solution of the Gauss' equations, the time of flight and Δv were defined for each transfer phase. A bi-objective optimisation mission cost function, based on these mission aspects was designed and exploited for both the single transfer optimisation and for the global sequence selection and optimisation. The combinatorial path optimisation problem was addressed through the development of a deterministic dynamic programming algorithm. This algorithm was selected for its computational performances and for its deterministic nature. The algorithm has been proven to be robust and to converge to the optimal solution of the problem.

Then, the whole developed algorithm was applied to a sub-set of the aforementioned population. The algorithm was proven to be fast converging to the solution and able to exploit the transfer strategy features in finding the optimal solution for each transfer. These features were critically analysed and justified. The field of multiple ADR trajectory and targets optimisation offers many possible future developments. Starting from the mission architecture, multiple different strategies can be developed and explored. For example, the removal kits could be dimensioned specifically for the targets, and their mass computation could be included in the mission optimisation. Moreover, in this work, aspects such as non-null orbit eccentricity of the targets and the phasing manoeuvres required were not directly addressed. Dropping these assumptions would improve the robustness of the method to different target's orbit and refine the transfer design. Clearly, complicating the model, could result in a reduced compatibility with the combinatorial path selection framework. A possible improvement would be to insert the application of a precise and defined ADR method to the model, including the proximity operations phase in the transfer optimisation. In this way, a parameter of merit indicating the compatibility with the specific removal method used could be defined for the debris selection. Similarly, also the introduction of an index of merit indicating the grade of danger caused by the presence of the debris in orbit could be inserted. Finally, the algorithm could be tested on different populations and number of debris, to compare and validate it with respect to other optimisation methods.

Acknowledgements

I thank the entire COMPASS research group for the possibility to work and research on this topic. In particular I want to thank Professor Colombo and Dr. Borelli for their constant and valuable support throughout all the research work.

References

[1] ESA. Space debris mitigation requirements. Technical report, ESA, 2023.

[2] A. M. Masserini. Design and optimization of an active debris removal service for large constellation, 2020. Master of Science in Space Engineering, Supervisor: Camilla Colombo, Co-supervisor: Simeng Huang.

[3] Medioni, Y. Gary, M. Monclin, C. Oosterhof, G. Pierre, T. Semblanet, P. Comte, and K. Nocentini. Trajectory optimization for multi-target active debris removal missions. Advances in Space Research, 72:2801–2823, 10 2023. ISSN 18791948. doi: 10.1016/j.asr.2022.12.013.

[4] M. C. Wijayatunga, R. Armellin, H. Holt, L. Pirovano, and A. A. Lidtke. Design and guidance of a multi-active debris removal mission. Astrodynamics, 7(4):383–399, 2023.

[5] Giulio Campiti. Resonant flybys in the b-plane: extension of the theory to elliptical planetary orbits and dynamic programming application, 2021. Master of Science in Space Engineering, Supervisor: Camilla Colombo, Co-supervisor: Alessandro Masat.

[6] M. Cerf. Multiple space debris collecting mission-debris selection and trajectory optimization. Journal of Optimization Theory and Applications, 156:761–796, 3 2013. ISSN 15732878. doi: 10.1007/s10957-012-0130-6.

[7] D. Madakat, J. Morio, and D. Vanderpooten. Biobjective planning of an active debris removal mission. Acta Astronautica, 84:182–188, 2013. ISSN 00945765. doi: 10.1016/j.actaastro.2012.10.038.

[8] A. Y. A. Naber. Debris sequence optimization for an active debris removal mission using a multi-indices rating system based algorithm, 2023. Master of Science in Space Engineering, Supervisor: Camilla Colombo, Co-supervisor: Giacomo Borelli.

[9] A. Barea, H. Urrutxua, and L. Cadarso. Optimal large-scale object selection and trajectory planning for active space debris removal missions. In 8th European Conference for Aeronautics and Space Sciences, 2019. doi: 10.13009/EUCASS2019-533.

[10] A. Barea, J. L. Gonzalo, C. Colombo, and H. Urrutxua. Preliminary analysis of an active debris removal mission for large constellations: A constraint programming methodology. In 5th International Workshop on Key Topics in Orbit Propagation Applied to SSA, Logrono, 2022.

[11] Marilena Di Carlo, Juan Manuel Romero Martin, and Massimiliano Vasile. Automatic trajectory planning for low-thrust active removal mission in low-earth orbit. Advances in Space Research, 59(5):1234–1258, 2017.

[12] F. Zuiani and M. Vasile. Extended analytical formulas for the perturbed Keplerian motion under a constant control acceleration. Celestial Mechanics and Dynamical Astronomy, 121:275–300, 3 2015. ISSN 15729478. doi: 10.1007/s10569-014-9600-5.

[13] J. Hon and M. R. Emami. Optimization framework for low-thrust active debris removal missions with multiple selected targets, 2022. URL www.amostech.com.

[14] Simeng Huang. Multi-Phase Mission Analysis and Design for Satellite Constellations with Low-Thrust Propulsion. PhD thesis, Politecnico di Milano, 2021. Supervisor: Camilla Colombo.

[15] V. Braun, A. Lüpken, S. Flegel, J. Gelhaus, M. Möckel, C. Kebschull, C. Wiedemann, and P. Vörsmann. Active debris removal of multiple priority targets. Advances in Space Research, 51:1638–1648, 5 2013. ISSN 02731177. doi: 10.1016/j.asr.2012.12. 003.

[16] ESA. Esa discos, 2023. https:// discosweb.esoc.esa.int/ [Accessed: 01 12-2023].